# Contents



# 1 INTRODUCTION

As molecules and heavy atoms get invoked for studies of fundamental interactions and properties, the demand for more accurate descriptions of the wavefunction within and close to the nucleus grow more stringent. With the generally increasing precision of quantum chemistry calculations, the simple point-nucleus approximation, resulting in the well-known $Z/r$ potential, is no longer completely adequate. The inadequacy becomes more and more evident as quantum chemistry takes on the challenge of molecules including heavy, or even superheavy, atoms: For large $Z$, the behaviour close to the nucleus becomes too singular for a point nuclear charge, and for the—still hypothetical—case of $Z > 137$, the Dirac equation breaks down. For finite nuclear distributions, the possible range extends much further.

Many properties depend on details of the nuclear structure. What are the alternatives for the nuclear distributions used in calculations? What are their advantages and disadvantages from a computational point of view? How should calculated results be presented in order to make possible meaningful comparisons between results obtained using different approaches? How much is known experimentally and how is that information best included in the calculations? These are a few of the questions addressed in this chapter.

This chapter focuses mainly on the distribution of charge, which, however influences also other properties. In Sec. 4 we give a brief discussion of physical effects close to the nucleus.

# 2 NUCLEAR CHARGE DISTRIBUTIONS

The early theorists, without access to computers, had strong reasons to use analytical descriptions of charge distributions and potentials, that enabled series expansions of analytical solutions of the wavefunctions within and close to the nucleus. A common choice was the homogeneous charge distribution inside a radius $R = R_0 A^{1/3}$, where $A$ is the mass number of nucleus. The most important parameter for many properties is the expectation value $\langle r^2 \rangle$ which has the value $3R^2/5$ for the homogeneous nucleus. Already this simple distribution gives the correct analytical behaviour of the electronic wavefunctions at $r = 0$ and has been used in many early analyses, and is discussed in more detail in Sec. 3.2. These expansions are also useful for a general understanding of the effects involved.

## 2.1 Experimental information

Experimental information about charge distributions are derived from many sources, including electron scattering. The experimental data indicate that $R_0 \simeq 1.2$ fm gives a reasonable approximation for the homogeneous distribution. Clearly, the tail of a real nucleus is less sharp than indicated by the homogeneous distributions. It is often described in terms of a "skin thickness" $t$, defined as the distance in which the charge density falls from 90% of its central value to 10%. Experiments indicate that $t$ is about 2.3 fm for most nuclei.

The primary data from electron scattering experiments are expressed in terms of a "Fourier-Bessel expansion". Figure 1 shows the resulting charge distribution for several different nuclei. It is possible to use these data directly, using a numerical approach, as shown in Sec. 3.1. Tabulations often give values relating to additional parameterizations, in particular the two and three-parameter Fermi distributions, as well as Gaussian expansions (de Vries, de Jager & de Vries 1987, Fricke, Bernhardt, Heilig, Schaller, Schellenberg, Schera & de Jager 1995), that are discussed in more detail below.

Another source are muonic X-ray energies. These probe somewhat different moments, the "Barrett moments" $\langle r^k e^{-\alpha r} \rangle$, of the nuclear distribution. Nevertheless, the results are quoted also in terms of $\langle r^2 \rangle$ (Engfer, Schneuwly, Vuilleumier, Walter & Zehnder 1974).

Optical isotope shifts provide an important source of complementary information, in particular for chains of radioactive isotopes. It is found that the changes in charge radius along an isotope chain are, in general, smaller than indicated by the textbook formula above. The isotope shifts also reveal an "odd-even staggering" of the $\langle r^2 \rangle$ values, providing evidence of nuclear shell structure (Aufmuth, Heilig & Steudel 1987*b*, Otten 1989). A spectacular recent application is the precision determination of the "deuteron structure radius" from the hydrogen-deuterim isotope shift of the 1s – 2s two-photon resonance (Huber, Udem, Gross, Reichert, Kourogi, Pachucki, Weitz & Hänsch 1998).

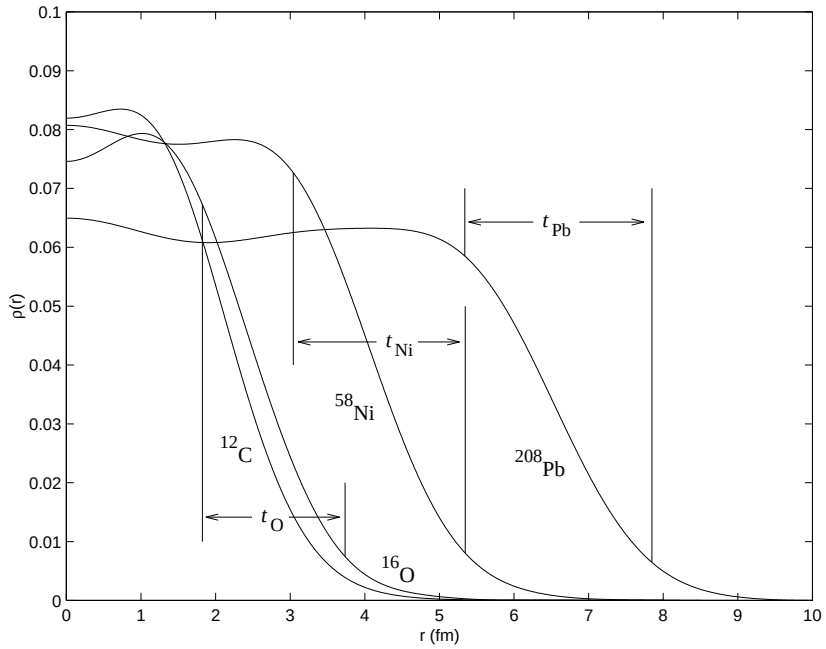


Figure 1: The radial charge distribution for several nuclei determined by electron scattering. The skin thickness $t$ is shown for O, Ni and Pb; its value is roughly constant at 2.3 fm. These distributions were obtained from Fourier-Bessel expansion data tabulated by de Vries, H., de Jager, C. W. & de Vries, C. (1987).

## 2.2 Nuclear distributions and electronic wavefunctions

The electrostatic potential energy, $V(r)$, for an electron in a spherically symmetric charge distribution, $\rho(r)$, is given by the well-known expression

$$V(r) = -\frac{e}{4\pi\epsilon_0}\left[\frac{4\pi}{r}\int_0^r \rho(r')r'^2\mathrm{d}r' - 4\pi\int_r^\infty \frac{1}{r'}\rho(r')r'^2\mathrm{d}r'\right] .$$

Outside the nucleus, this expression reduces to the same potential, $-Ze^2/4\pi\epsilon_0 r$, as from a point nucleus. For a homogeneous distribution, where $\rho(r) = 3Ze/4\pi R^3$ within a nuclear radius $R$, the electrostatic potential for $r \leq R$ is

$$V(r) = -\frac{1}{4\pi\epsilon_0}\frac{Ze^2}{r}\left(\frac{3r}{2R} - \frac{r^3}{2R^3}\right) . \qquad (1)$$

We note that the potential is essentially constant at $V_0 = -(1/4\pi\epsilon_0)\times(3Ze^2/2R)$ very close to the origin. This determines the behaviour of the orbitals for very small $r$, which is obtained by a series expansion of the coupled radial equations

from the Dirac equation:

$$
\begin{aligned}
-\hbar c \left[\frac{\mathrm{d}}{\mathrm{d}r} - \frac{\kappa}{r}\right] G(r) &= [\varepsilon - V(r)]\, F(r)\,, \\
\hbar c \left[\frac{\mathrm{d}}{\mathrm{d}r} + \frac{\kappa}{r}\right] F(r) &= \left[\varepsilon + 2m_{\mathrm{e}}c^2 - V(r)\right] G(r)\,, \qquad (2)
\end{aligned}
$$

where $\kappa = \mp(j+1/2)$ for $j = l \pm 1/2$, $\varepsilon$ is the binding energy and $F(r)$ and $G(r)$ are the radial parts of the "large" and "small" components, respectively, of a relativistic wavefunction. (The sign relation in Eq. (2) between $F$ and $G$ is valid for the "$ls$-convention" for the coupling of spin and orbital angular momentum.)

Below, we use atomic units, where $e = m_{\mathrm{e}} = 4\pi\epsilon_0 = \hbar = 1$ and $c = 1/\alpha \approx 137$. (A word of caution is in place: Relativistic atomic calculations form a meeting ground between traditional atomic and molecular calculations and field theoretical approaches, where the equations are instead expressed in "natural units", where $c = m_{\mathrm{e}} = 4\pi\epsilon_0 = \hbar = 1$ and $e^2 = \alpha \approx 1/137$).

For a point nucleus, the leading term is $r^\gamma$, where $\gamma = \sqrt{\kappa^2 - (Z\alpha)^2}$, for both $F(r)$ and $G(r)$.The solution $r^{-\gamma}$ is singular for $r = 0$ and must be rejected for point nuclei. For an extended nucleus, however, this term enters with a small coefficient in the matching of outer and inner solutions.

Inside an extended nucleus the leading term in the upper component is $r^l$. For $j = l + 1/2$ orbitals, the lower component carries an extra factor $r$, whereas for the $j = l - 1/2$ orbitals, the lower component has a small term $r^{l-1}$ which dominates for very small $r$.

We note that atomic orbitals with $j = 1/2$ (i.e. s and $\mathrm{p}_{1/2}$) have an appreciable probability within the nucleus, where their density is essentially constant. The effect of the nuclear distribution on atomic properties then becomes proportional to the expectation value, $\langle r^2 \rangle = \int r^2 \rho(\boldsymbol{r}) \mathrm{d}V / \int \rho(\boldsymbol{r}) \mathrm{d}V$, of the nuclear distribution. This observation is well-known from studies of optical isotope shifts, which are changes in transition frequency between different isotopes of an element. The "field" or "volume" isotope shift is the part due to the different charge distributions and is expressed as $\delta\nu = F\delta\langle r^2 \rangle$, where $F = (2\pi/3)(Ze^2/4\pi\epsilon_0)\Delta|\Psi(0)|^2$.

For heavy nuclei, also the next terms in the expansion of the wavefunctions become significant. Thus, also higher moments, $\delta\langle r^4 \rangle$, $\delta\langle r^6 \rangle$, ... of the nuclear distribution contribute. As an illustration, Fig. 2.2, shows the 1s energy for hydrogen-like Bi ($Z = 83$) for Fermi distributions with various values of $\langle r^2 \rangle$ and the "skin-thickness".

The electron density then varies within the nucleus, giving contributions from higher moments, These "Seltzer correction" (Seltzer 1969) can be accounted for by including a factor $\kappa$ which is e.g. about 0.92 for Bi (Torbohm, Fricke & Rosén 1985). These factors are of course not needed if the distribution is included directly in the calculation.

Below, we consider in more detail the expression for potentials and orbitals for homogeneous, Fermi and Gaussian models of the nuclear distributions. Several other distributions have been considered in detail by Andrae (Blundell,

Baird, Botham, Palmer, Stacey & Woodgate 2000), who provides expressions for wave functions and energy corrections for a wide range of nuclear distributions, as well as a comparison of first-order energy corrections for one-electron systems with exact ones for non-relativistic and relativistic treatments.

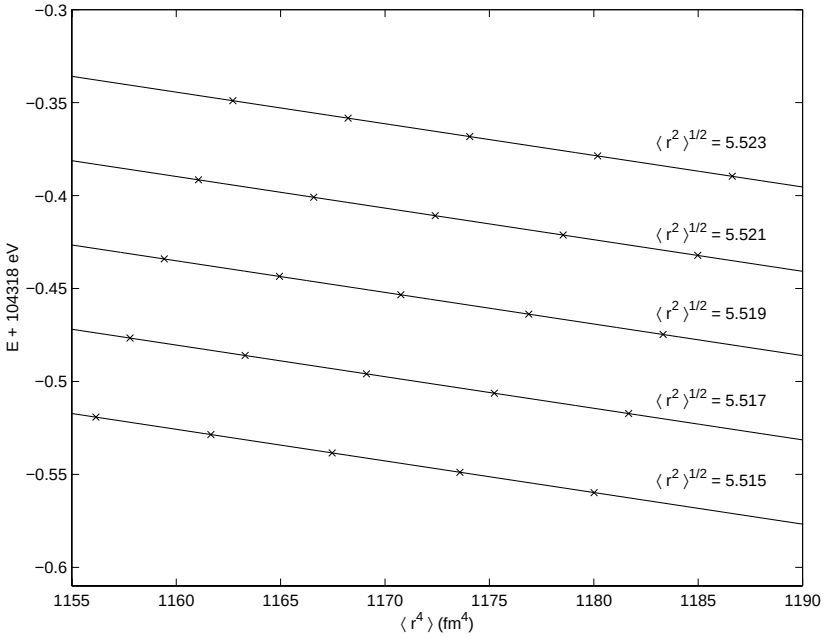


Figure 2: The dependence of the ground state energy of hydrogen-like bismuth on the nuclear charge distribution. The lines show results for constant values of the nuclear rms-radius, and were obtained by fitting a linear expansion in $\langle r^4 \rangle$ to the results of explicit numerical calculations (marked by crosses) for different values of the nuclear parameters

# 3 FINITE NUCLEAR CHARGE DISTRIBUTIONS

In this section we give a brief presentation of models commonly used to account for the experimentally obtained information about the nuclear distribution. We also present the resulting potential, and discuss the related initial conditions and orbital behaviour for small $r$ values.

## 3.1 Electron Scattering and The Fourier-Bessel expansion

The data from electron scattering are analyzed using the Plane Wave Born Approximation, and the charge distribution is obtained as the Fourier transform of the form factors $F(q)$, giving, for a spherically symmetric charge distribution

$$\rho(r) = \frac{1}{2\pi^2} \int F(q) \frac{\sin(qr)}{qr} q^2 \mathrm{d}q \,.$$

The accuracy is limited by the finite range of $q$ values. The Fourier-Bessel analysis, introduced by Dreher and coworkers (Dreher, Friedrich, Merle, Rothhaas & Lührs 1974), assumes a cutoff radius for the nucleus and uses an analytical approximation for the form factor $F(q)$ for $q$ values beyond the maximum available value. The charge distribution is then written as

$$\rho(r) = \begin{cases} \sum_\nu a_\nu j_0\left(\frac{\nu\pi r}{R}\right) & \text{for} \quad r \le R \\ 0 & \text{for} \quad r > R \,, \end{cases}$$

where $j_0(x) = \sin(x)/x$ is the zeroth order spherical Bessel function. The first few coefficients are deduced from experiments and given in tabulations (de Vries et al. 1987, Fricke et al. 1995).

The expressions for the total charge, $Q$, and the potential energy $V(r)$ are

$$\begin{aligned} Q &= 4\pi \sum_\nu a_\nu \left(\frac{R}{\nu\pi}\right)^3 \nu\pi(-1)^{\nu+1} \,, \\ V(r) &= \begin{cases} -4\pi \sum_\nu a_\nu \left(\frac{R}{\nu\pi}\right)^2 \left[ j_0\left(\frac{\nu\pi r}{R}\right) - (-1)^\nu \right] & \text{for} \quad r \le R \\ -\frac{Z}{r} & \text{for} \quad r > R \,. \end{cases} \end{aligned}$$

This potential has been applied in the case of the ground-state hyperfine structure of hydrogen-like Bi (Gustavsson & Mårtensson-Pendrill 1998).

The second moment, $\langle r^2 \rangle$, of the charge distribution can also be expressed in terms of the Fourier-Bessel parameters:

$$\langle r^2 \rangle = \frac{4\pi}{Q} \sum_\nu a_\nu \left(\frac{R}{\nu\pi}\right)^5 \nu\pi(-1)^\nu \left[6 - (\nu\pi)^2\right]$$

and is usually quoted in tabulations, as well as values for the Fermi and Gaussian parametrizations, that are discussed later.

## 3.2 Uniform distribution and orbital expansions

The uniform distribution of charge within a radius, $R$ was discussed briefly in Sec. 2.2. Obviously, there is a discontinuity in the charge distribution, $\rho(r)$, at the nuclear boundary leading to a discontinuity in the second derivative of the potential at $r = R$. Care must thus be taken in numerical integration schemes to

avoid spurious effects related to the nuclear boundary. In numerical approaches the discontinuity also leads to slower convergence with the grid spacing (Visscher & Dyall 1997).

To find a detailed description for the orbital behaviour for very small $r$, a power series Ansatz for the orbitals is inserted together with the expression for the potential [Eq. (1)] in the radial Dirac equation [Eq. (2)].

To facilitate the notation in the orbital expansion, we write the potential in the form $V(r,R) = V_0 + V_2 r^2$, where $V_0 = -3Z/2R$ and $V_2 = -V_0/3R^2$ for the homogeneous distribution. The other potentials discussed below lead, in addition, to terms of the type $V_3 r^3$ and higher, which affect the higher-order terms in the series expansion of the orbitals. Using these parameters and the binding energy, $\epsilon$, and keeping the lowest-order terms gives for $\kappa < 0$

$$\begin{aligned} F(r) &= N\left\{ r^{|\kappa|} - \frac{(\varepsilon - V_0)(\varepsilon + 2c^2 + V_0)}{2c^2(1+2|\kappa|)} r^{|\kappa|+2} \dots \right\} , \\ G(r) &= N\left\{ -\frac{(\varepsilon - V_0)}{c(1+2|\kappa|)} r^{|\kappa|+1} \right. \\ &\quad \left. + \left[ \frac{(\varepsilon - V_0)^2(\varepsilon + 2c^2 + V_0)}{2c^3(1+2|\kappa|)(3+2|\kappa|)} + \frac{V_2}{c(3+2|\kappa|)} \right] r^{|\kappa|+3} \dots \right\} , \end{aligned}$$

and for $\kappa > 0$

$$\begin{aligned} F(r) &= N\left\{ r^{\kappa+1} \right. \\ &\quad \left. - \left[ \frac{(\varepsilon - V_0)(\varepsilon + 2c^2 - V_0)}{2c^2(3+2\kappa)} + \frac{V_2(1+2\kappa)}{(\varepsilon + 2c^2 - V_0)(3+2\kappa)} \right] r^{\kappa+3} \dots \right\} , \\ G(r) &= N\left\{ \frac{c(1+2\kappa)}{\varepsilon + 2c^2 - V_0} r^{\kappa} - \frac{\varepsilon - V_0}{2c} r^{\kappa+2} \dots \right\} , \end{aligned}$$

where $N$ is a normalizing constant.

The energy dependence of these expressions is very weak, since the binding energy $\varepsilon$ is much smaller than the potential energy, $V_0 = -3Z/2R$ at $r = 0$, in particular for low $Z$.

### 3.3 Fermi distribution

The two-parameter Fermi model gives a realistic description of the nuclear distribution (Hofstadter, Fechter & McIntyre 1953, Hahn, Ravenhall & Hofstadter 1956), and at the same time provides considerable flexibility in the analysis:

$$\rho(r) = \frac{\rho_0}{1 + \mathrm{e}^{(r-c)/a}} , \tag{3}$$

where, $c$ is the half-density radius and $a$ is related to the skin thickness $t$ by $t = (4 \ln 3)a$, giving values of $a$ roughly constant at 0.524 fm. For vanishing skin thickness, the Fermi form reduces to the homogeneous distribution with a radius $R = c$.

The shape of the Fermi distribution is identical to that of the Woods-Saxon potential. The analogy between the nuclear distribution and potential is related to the short-range character of the strong interaction, which holds the nucleus together.

The shape of an arbitrary nuclear distribution can often be adequately described by the moments $\langle r^{2n} \rangle$ of the distribution. Varying the parameter in the Fermi distribution makes it possible to study the influence of the higher nuclear moments, $\langle r^{2n} \rangle$, given to a good approximation (Gustavsson & Mårtensson-Pendrill 1998), by the relations

$$\begin{aligned}
\langle r^2 \rangle &\approx \frac{3}{5}c^2 + \frac{7}{5}\pi^2 a^2 \,, \\
\langle r^4 \rangle &\approx \frac{3}{7}c^4 + \frac{18}{7}\pi^2 a^2 c^2 + \frac{31}{7}\pi^4 a^4 \,, \\
\langle r^6 \rangle &\approx \frac{3}{9}c^6 + \frac{11}{3}\pi^2 a^2 c^4 + \frac{239}{15}\pi^4 a^4 c^2 + \frac{127}{5}\pi^6 a^6 \,.
\end{aligned}$$

The electrostatic potential cannot be obtained analytically for the Fermi distribution Eq. (3). However, convenient expressions for the evaluation of the potential have been derived (Parpia & Mohanty 1992) and are used in the procedure adopted in the general atomic structure package of computer programs GRASP$^2$ (Dyall, Grant, Johnson, Parpia & Plummer 1989, Parpia & Grant 1991), and are summarized briefly below.

The radial integrals can be written in terms of infinite series, that converge to machine precision with just a few terms included. The potential energy for $r < c$ can be written as

$$\begin{aligned}
V_{r<c}(r) &= -\frac{N}{r}\left[\frac{3r}{2c} - \frac{r^3}{2c^3} + \frac{r\pi^2 a^2}{2c^3} - \frac{3ra^2}{c^3}S_2\left(\frac{r-c}{a}\right) + \frac{6a^3}{c^3}S_3\left(\frac{r-c}{a}\right)\right. \\
&\quad \left. - \frac{6a^3}{c^3}S_3\left(-\frac{c}{a}\right)\right] \,,
\end{aligned}$$

and for the case $r > c$ we have

$$\begin{aligned}
V_{r>c}(r) &= -\frac{N}{r}\left[1 + \frac{\pi^2 a^2}{c^2} + \frac{3ra^2}{c^3}S_2\left(-\frac{r-c}{a}\right) + \frac{6a^3}{c^3}S_3\left(-\frac{r-c}{a}\right)\right. \\
&\quad \left. - \frac{6a^3}{c^3}S_3\left(-\frac{c}{a}\right)\right] \,,
\end{aligned}$$

where the $S_k$ functions are given by

$$S_k(x) = \sum_{n=1}^{\infty}(-1)^n \frac{\mathrm{e}^{xn}}{n^k} \,,$$

and the normalization condition gives

$$N = \frac{Z}{\left[1 + \frac{\pi^2 a^2}{c^2} - \frac{6a^3}{c^3}S_3\left(-\frac{c}{a}\right)\right]} \,.$$

In the expression for the potential within the nucleus, we regognize the constant term $V_0 = -3Z/2c$ from the uniform distribution for the case of vanishing skin thinkness.

### 3.3.1 Deformed nuclei

Generalizations of the Fermi model to describe deformed nuclei have been applied e.g. in the study of energies for highly charged uranium (Indelicato & Lindroth 1992, Ynnerman, James, Lindgren, Persson & Salomonson 1994). The nuclear radius parameter $c$ in the Fermi distribution Eq. (3.3) is then replaced by

$$R(\boldsymbol{r}) = c\left[1 + \beta_2 Y_{20}(\boldsymbol{r}) + \beta_4 Y_{40}(\boldsymbol{r})\right], \tag{4}$$

which includes an explicit dependence on the angular coordinates.

### 3.3.2 The three-parameter Fermi model

The three-parameter Fermi distribution makes it possible to reproduce the small dip, found in the charge distribution for small $r$, as seen in Fig. 1.

## 3.4 Gaussian expansions

Many quantum chemistry programs expand the electronic wavefunctions in terms of Gaussian-type functions. Using a Gaussian charge distribution then has the advantage to make it possible to evaluate electron-nucleus interactions using the same integral routines as the electron-electron interactions. Visscher and Dyall (Visscher & Dyall 1997) in their comparison of different approaches use a one-parameter Gaussian distribution $\rho(r) = Z\left(\xi/\pi\right)^{3/2}\exp(-\xi/r^2)$ where the width is determined from the experimental rms radius: $\xi = 3/\langle 2R^2\rangle$, giving a potential related to the error function: $V(r) = -(Z/r) \times \mathrm{erf}\left(\sqrt{\xi}r\right)$. Visscher and Dyall found that this one-parameter Gaussian potential reproduced about 99% of the correction to the energies for high $Z$, whereas the uniform distribution gave about about 100.1% of the correction, indicating the importance of the higher $\langle r^{2n}\rangle$ moments.

In order to obtain a model-independent fit of the charge distribution, a parameterization of the experimental data into a sum of Gaussians, which was suggested by (Sick 1974). The width $\gamma$ of the Gaussians is chosen to be equal to the smallest width of the peaks in the nuclear radial wavefunctions calculated by the Hartree-Fock method. Only positive values of the amplitudes of the Gaussians are allowed so that no structures narrower than $\gamma$ can be created through interference. An advantage of the use of Gaussians is that values of $\rho(r)$ at different values of $r$ are decoupled to a large extent because of the rapid decrease of the Gaussian tail. The charge distribution is then expressed as

$$\rho(r) = \sum_i A_i \left\{ \mathrm{e}^{-[(r-R_i)/\gamma]^2} + \mathrm{e}^{-[(r+R_i)/\gamma]^2} \right\},$$

where the coefficients $A_i$ are given by

$$A_i = \frac{ZeQ_i}{2\pi^{3/2}\gamma^3\,(1+2R_i^2/\gamma^2)}\ .$$

In this definition the values of $Q_i$ indicate the fraction of the charge contained in the $i$th Gaussian, normalized such that

$$\sum_i Q_i = 1\ .$$

The second term for each parameter, centered around a non-physical negative $R_i$ value is included to ensure that the slope of the distribution is indentically zero at the origin. An additional advantage over the Foourier-Bessel expansion is that the Sum-over Gaussians by construction gan give only non-negative values for $\rho(r)$.

The relevant parameters can, as in the case of the Fourier-Bessel expansion, be found tabulated (de Vries et al. 1987, Fricke et al. 1995). For high-spin nuclei it might be valuable to include an angular dependence in analogy with Eq. (4). In general, they give a better description of the inner part of the nucleus better than the Fourier-Bessel expansion, which on the other hand, gives a better description in the outer part where the Gaussian tail decays too rapidly. Since an electronic wave function is more sensitive to the outer part of the nuclear distribution the Fourier-Bessel expansion is preferable. On the other hand, the main part of the energy correction (which in itself is only 0.12% for $Z = 100$) is accounted for already with the one-parameter Gaussian potential, so the Gaussian expansion should clearly be adequate for most applications.

# 4 PHYSICS NEAR THE NUCLEUS

The energy of a system is only weakly influenced by details in the nuclear charge distribution. Even for $Z = 100$, using an extended nuclear charge gives only an 0.1% reduction of the binding energy. Differences between different distributions are less than a percent of the correction itself. However, several atomic properties depend directly on the wavefunction close to the nucleus. Using a point charge, with the resulting unphysical behaviour of the wavefunction at $r = 0$ then leads to overestimates by several percent, for high Z.

An important observation for the study of nuclear properties is that the orbital behaviour within the nucleus depends on the angular momentum, but is essentially independent of the binding energy. For very heavy nuclei, the binding energies are a larger fraction of the nuclear potential energy, giving a small $n$-dependence in the orbital behaviour close to the nucleus, as demonstrated e.g. by Shabaev (Shabaev 1994) for hyperfine structure corrections for different values of Z.

For a many-electron system, all electrons are affected, but mainly through their interaction with the modified $j = 1/2$ orbitals. It is then the sensitivity of

the interaction of the $j = 1/2$ orbitals that needs to be studied in detail. A striking illustration is the comparison by Visscher and Dyall (1997) of the relation between the corrections for the 1s orbital energy and the total energy. The ratio between the corrections to the point nuclear value for Fermi, homogeneous and Gaussian distribution were plotted for both cases, giving two figures differing only in their captions. In this way, nuclear size effects obtained for one charge distribution could be rescaled to another distribution by applying correction factors determined from the effects on the $s$ orbitals. (The difference between the higher moment contributions for s and $p_{1/2}$ is relatively insignificant.)

As discussed in previous sections, the shape can be parameterized in terms of the moment $\langle r^2 \rangle$, $\langle r^4 \rangle$ and $\langle r^6 \rangle$ of the nuclear charge. To facilitate comparisons between different calculations, we therefore suggest that whatever nuclear distribution is used, these moments should be given (or sufficient information provided to make their extraction easy).

## 4.1 Hyperfine structure

The best known example of nuclear structure effects in atomic spectra is the magnetic hyperfine structure (hfs), which arises from a coupling between the magnetic moments of the nucleus and the electron, given by

$$h_{\rm p}^{{\rm h}fs} = \hat{r} \cdot \frac{\boldsymbol{\mu} \times \boldsymbol{\alpha}}{r^2}$$

for a point magnetic dipole.

The resulting energy splitting is often expressed as $A\mathbf{I} \cdot \mathbf{J}$ , where $I$ and $J$, are the spins of the nucleus and the electron, respectively. The hfs was an early source of information about nuclear spin, magnetic moments. In general, magnetic moments are known better through other sources, such as NMR. Hyperfine structure can thus be used in order to test atomic wavefunctions (Safronova, Johnson & Derevianko 1999).

The ratio between the magnetic moment and the "A-factor" is, however, found to vary slightly between various isotopes of an element. Part of this "hyperfine anomaly" arises from differences in the charge distribution (the so-called Breit-Rosenthal effect). Another contribution to the hyperfine anomaly, the "Bohr-Weisskopf effect" arises from the distribution of nuclear magnetic moment. In this way, the hyperfine anomaly can give information about magnetic moment distribution.

## 4.2 Parity non-conserving operators

The study of parity non-conserving weak interaction has been a fruitful branch of atomic physics. Recent experiments for Cs are accurate at the percent level, providing a serious challenge to atomic theory. The electro-weak interaction involves the neutron distribution and James and Sandars (James & Sandars 1999) have analysed in detail the sensitivity to details in the distribution. Experimental information can possibly be obtained from hyperfine anomalies, as in

the recent experiments for Fr isotopes (Grossman, Orozco, Pearson, Simsarian, Sprouse & Shao 1999).

The near energy-independence of the orbital shape close to the nucleus forms the basis for derivations of relations between different interactions close to the nucleus, by using the series expansion of the wavefunction. The ratios are, of course, modified by many-body corrections if the operators have different angular structure, as discussed e.g. in (Mårtensson-Pendrill, Pendrill, Salomonson, Ynnerman & Warston 1990). This has long been used to estimate field isotope shifts from observed hyperfine structures. (Kopfermann 1958, Aufmuth, Heilig & Steudel 1987*a*) and more recently for various $P$ and $T$ violating operators (Sushkov, Flambaum & Khriplovich 1984, Mårtensson-Pendrill 1992). The "Schiff moments", e.g., involve the difference between the charge and electric dipole distributions.

As quantum chemists approach systems with increasingly heavy atoms, the use of an extended charge distribution becomes essential, and the charge distribution used must be clearly specified to make possible comparison of different results.

# References


Aufmuth, P., Heilig, K. & Steudel, A. (1987*a*), '??', *At. Data Nucl. Data Tables* **37**, 455.

Aufmuth, P., Heilig, K. & Steudel, A. (1987*b*), 'Changes in Mean-Square Nuclear Charge Radii from Optical Isotope Shifts', *Atomic Data and Nuclear Data Tables* **37**(3), 455–490.

Blundell, S. A., Baird, P. E. G., Botham, C. P., Palmer, C. W. P., Stacey, D. N. & Woodgate, G. K. (2000), 'Finite nuclear charge density distributions in electronic structure calculations for atoms and molecules', *Physics Report* **??**, ??

de Vries, H., de Jager, C. W. & de Vries, C. (1987), 'Nuclear Charge-Density-Distribution Parameters from Elastic Electron Scattering', *Atomic Data and Nuclear Data Tables* **36**(3), 495–536.

Dreher, B., Friedrich, J., Merle, K., Rothhaas, H. & Lührs, G. (1974), 'The determination of the nuclear ground state and transition charge density from measured electron scattering data', *Nuclear Physics* **A235**(1), 219–248.

Dyall, K. G., Grant, I. P., Johnson, C. T., Parpia, F. A. & Plummer, E. P. (1989), 'GRASP: a general-purpose relativistic atomic structure program', *Computer Physics Communications* **55**(3), 425–456.

Engfer, R., Schneuwly, H., Vuilleumier, J. L., Walter, H. K. & Zehnder, A. (1974), 'Charge-Distribution Parameters, Isotope shifts, Isomer shifts, and

Magnetic Hyperfine Constants from Muonic Atoms', *Atomic Data and Nuclear Data Tables* **14**(5–6), 509–597.

Fricke, G., Bernhardt, C., Heilig, K., Schaller, L. A., Schellenberg, L., Schera, E. B. & de Jager, C. W. (1995), 'Nuclear Ground State Charge Radii from Electromagnetic Interactions', *Atomic Data and Nuclear Data Tables* **60**(2), 177–285.

Grossman, J. S., Orozco, L., Pearson, M., Simsarian, J. E., Sprouse, G. D. & Shao, W. Z. (1999), 'Hyperfine anomaly measurements in francium isotopes and the radial distribution of neutrons', *Phys. Rev. Lett.* **83**, 935–938.

Gustavsson, M. G. H. & Mårtensson-Pendrill, A.-M. (1998), 'Four Decades of Hyperfine Anomalies', *Advances in Quantum Chemistry* **30**, 343–360.

Hahn, B., Ravenhall, D. G. & Hofstadter, R. (1956), 'High-Energy Electron Scattering and the Charge Distributions of Selected Nuclei', *Physical Review* **101**(3), 1131–1142.

Hofstadter, R., Fechter, H. R. & McIntyre, J. A. (1953), 'High-Energy Electron Scattering and Nuclear Structure Determinations', *Physical Review* **92**(4), 978–987.

Huber, A., Udem, T., Gross, B., Reichert, J., Kourogi, M., Pachucki, K., Weitz, M. & Hänsch, T. W. (1998), 'Hydrogen-Deuterium 1S–2S Isotope Shift and the Structure of the Deuteron', *Physical Review Letters* **80**(3), 468–471.

Indelicato, P. & Lindroth, E. (1992), 'Relativistic effects, correlation, and QED corrections on $K\alpha$ transitions in medium to very heavy atoms', *Physical Review A* **46**(5), 2426–2436.

James, J. & Sandars, P. G. H. (1999), 'A parametric approach to nuclear size and shape in atomic parity nonconservation', *J. Phys. B* **32**, 3295–3307.

Kopfermann, H. (1958), *Nuclear Moments*, Academic Press, New York.

Mårtensson-Pendrill, A.-M. (1992), Calculations of P and T violating properties in atoms and molecules, *in* S. Wilson, ed., 'Methods in Computational Chemistry', Vol. 5, Plenum Press, New York, pp. 99–156.

Mårtensson-Pendrill, A.-M., Pendrill, L., Salomonson, S., Ynnerman, A. & Warston, H. (1990), 'Reanalysis of the isotope shift and nuclear charge radii in radioactive potassium isotopes', *J. Phys. B* **23**, 1749–1761.

Otten, E. W. (1989), 'Nuclear Radii and Moments of Unstable Isotopes', *Treatise on Heavy-Ion Science* **8**, 517–638.

Parpia, F. A. & Grant, I. P. (1991), 'Software for relativistic atomic theory: the GRASP project at Oxford', *Journal de Physique IV* **1**(C1), 33–46.

Parpia, F. A. & Mohanty, A. K. (1992), *Phys. Rev. A* **46**, 3735.

Safronova, M. S., Johnson, W. & Derevianko, A. (1999), 'Relativistic many-body calculations of energy-levels, hyperfine constants, electric dipole matrix elements, and static polarizabilities for alkali-metal atoms', *Phys. Rev. A* **60**, 4476–4487.

Seltzer, E. C. (1969), '$K$ X-Ray Isotope Shifts', *Physical Review* **188**(4), 1916–1919.

Shabaev, V. M. (1994), 'Hyperfine structure of hydrogen-like ions', *J. Phys. B* **27**, 5825–5832.

Sick, I. (1974), 'Model-independent nuclear charge densities from elastic electron scattering', *Nuclear Physics* **A218**(3), 509–541.

Sushkov, O., Flambaum, V. V. & Khriplovich, I. B. (1984), '??', *Sov. Phys. JETP* **60**, 873–883.

Torbohm, G., Fricke, B. & Rosén, A. (1985), 'State-dependent volume isotope shifts of low-lying states of group-II*a* and -II*b* elements', *Physical Review A* **31**(4), 2038–2053.

Visscher, L. & Dyall, K. G. (1997), 'Dirac-Fock Atomic Electronic Structure Calculations Using Different Nuclear Charge Distributions', *Atomic Data and Nuclear Data Tables* **67**(2), 207–224.

Ynnerman, A., James, J., Lindgren, I., Persson, H. & Salomonson, S. (1994), 'Many-body calculation of the $2p_{1/2,3/2}$-$2s_{1/2}$ transition energies in Li-like $^{238}$U', *Physical Review A* **50**(6), 4671–4678.